ACS APPLIED MATERIALS & INTERFACES

Research Article

www.acsami.org

Fumed Silica-Based Single-Ion Nanocomposite Electrolyte for Lithium Batteries

Hui Zhao,[†,§] Zhe Jia,[†,§] Wen Yuan,[†] Heyi Hu,[‡] Yanbao Fu,[†] Gregory L. Baker,[‡] and Gao Liu*[,†]

[†]Energy Storage and Distributed Resources Division, Energy Technologies Area, Lawrence Berkeley National Laboratory, Berkeley, California 94720, United States

[‡]Department of Chemistry, Michigan State University, East Lansing, Michigan 48824, United States

Supporting Information

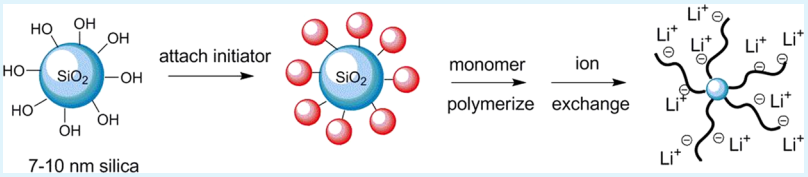

ABSTRACT: A composite lithium electrolyte composed of polyelectrolyte-grafted nanoparticles and polyethylene glycol dimethyl ether (PEGDME) is synthesized and characterized. Polyanions immobilized by the silica nanoparticles have reduced anion mobility. Composite nanoparticles grafted by poly(lithium 4-styrenesulfonate) only have moderate conductivity at 60 °C. Almost an order increase of the conductivity to ~10^{-6} S/cm is achieved by co-polymerization of the poly(ethylene oxide) methacrylate with sodium 4-styrenesulfonate, which enhances dissociation between lithium cation and polyanion and facilitates lithium ion transfer from the inner part of the polyelectrolyte layer. This composite electrolyte has the potential to suppress lithium dendrite growth and enable the use of lithium metal anode in rechargeable batteries.

KEYWORDS: *polymer-grafted silica nanoparticle, transference number, solid-state electrolyte, lithium battery, poly(ethylene oxide)*

INTRODUCTION

Lithium ion batteries (LIBs) have enabled the development of a variety of portable electronic devices, stationary grid-energy storage components, and hybrid/electric vehicles.[1,2] However, the low energy density of LIBs has been the bottleneck for the replacement of internal combustion vehicles by battery-powered electric vehicles.[3−6] Lithium metal is the most promising anode for a rechargeable battery, with a theoretical capacity of 3860 mAh/g, which 10 times larger than the state-of-art graphite anode (372 mAh/g).[7] The successful application of lithium metal anode will also open up the opportunities for other high-energy chemistries such as lithium air (O_2) and lithium sulfur batteries. Also, from the perspective of manufacturing, the ductile lithium metal is promising for large-scale production as battery anode materials.[8] Thus, a reliable rechargeable lithium metal battery has attracted attention from both academia and industry. However, the use of liquid electrolyte in contact with the lithium metal leads to irregular electrodeposition of metallic lithium;[9,10] this causes serious hazardous issues.[11] Zhang et al. showed that the use of selected cations such as cesium or rubidium ions was able to force the deposition of lithium to adjacent regions of the lithium metal anode and eliminate dendrite formation.[12,13] Cui et al. deposited a monolayer of interconnected amorphous hollow carbon nanospheres, which isolated the lithium metal depositions and enabled the formation of a stable solid electrolyte interphase (SEI).[14]

Solid-state polymer electrolyte (SPE) with high mechanical modulus and high lithium transference number, on the other hand, proposes a promising solution to prevent lithium dendrite formation and potentially address safety issues related to the use of liquid electrolytes.[15] Chazalviel proposed that electrolytes with high conductivity and reduced anion mobility could suppress the growth of lithium dendrite, which help avoid the decreased concentration gradient of the electrolyte.[16] Poly(ethylene oxide) (PEO) with dopant lithium salts, such as $LiPF_6$,[17] LiBOB, $LiCF_3SO_3$, and $Li[N(SO_2CF_3)_2]$ (LiTFSI),[18] have been widely used as solid polymeric electrolytes. Mobile ions generated from these dopant salts have typical lithium transference numbers (t_{Li^+}) of 0.1−0.3; anion is the dominant species in the ionic conductivity of lithium electrolytes.[19] An effective approach of increasing lithium transference number is to chemically attach the anions on the polymer backbone and limit anion mobility. Structurally this material contains only one mobile charge, which is the lithium cation dissociated from the anion.[20−24] Previously, a monolayer of anions was attached to the surface of a silica nanoparticle.[25,26] A silica polymer composite also has better mechanical property than that of the pure PEO.[27,28] However, decorating particle surfaces with a monolayer of anions

Received: June 18, 2015
Accepted: August 12, 2015
Published: August 12, 2015

ACS Publications © 2015 American Chemical Society

DOI: 10.1021/acsami.5b05419
ACS Appl. Mater. Interfaces 2015, 7, 19335−19341

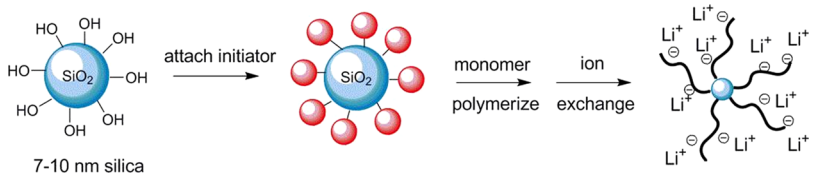

Figure 1. Synthetic approach for polyelectrolyte-decorated nanoparticles.

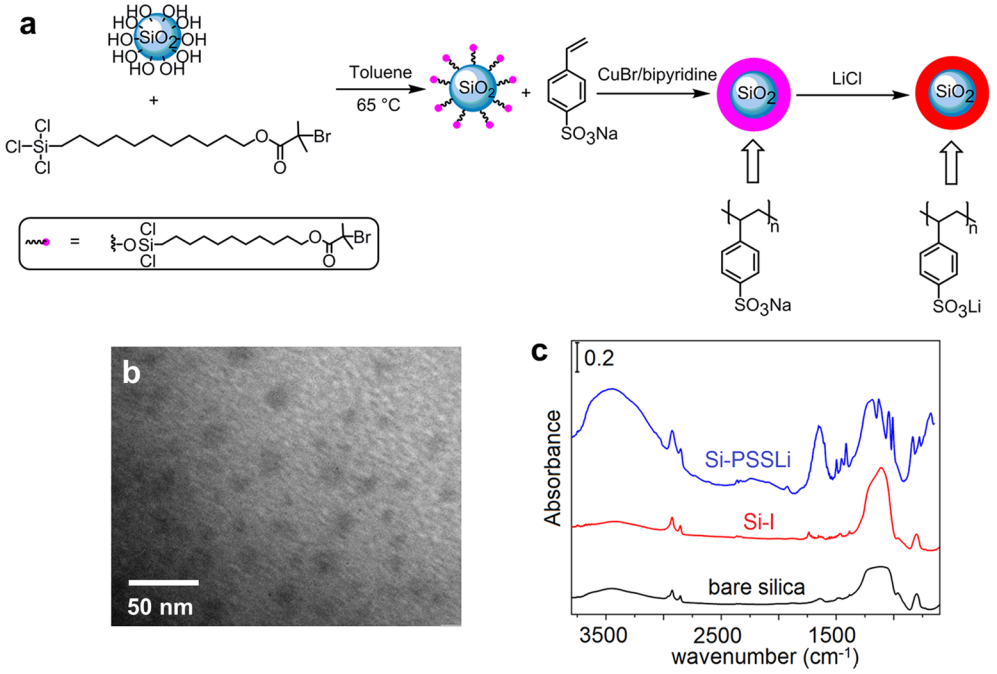

Figure 2. (a) Surface ATRP of sodium 4-styrenesulfonate on silica particle (Si-PSSNa) and lithiation to Si-PSSLi. (b) TEM image of Si-PSSLi. (c) FTIR spectra of bare silica nanoparticles, Si-initiator, and Si-PSSLi.

provides too few anions to support high conductivity in a bulk electrolyte (O/Li ratio = 120).

An alternative approach to increasing anion concentrations is to move from monolayer coverage of particles to polyelectrolytes anchored to the fumed silica particle surfaces (Figure 1). In principle, growing polymers from particle surfaces, especially by controlled polymerization methods, such as atom transfer radical polymerization (ATRP), will increase the carrier concentration near the carrier concentration of the bulk polyelectrolyte. The research described in this work focuses on nanoparticle systems where lithium counteranions are immobilized on polyelectrolytes grown from nanoparticles. A low molecular weight (M_w = 500 g/mol) polyethylene glycol dimethyl ether (PEGDME) is used for lithium ion transport.

EXPERIMENTAL SECTION

Materials. Snowtex-S (7−10 nm) silica nanoparticle sample is a gift from Nissan Chemical. Cu^{I}Br (Aldrich, 99.999%) is purified using saturated aqueous sodium bromide solution. Bipyridine (Aldrich, 99%) is recrystallized from hexane and sublimed prior to use. Poly(ethylene glycol) methyl ether methacrylate (PEGMA) (average M_n = 1100; Aldrich) is passed through a basic alumina column to remove the inhibitor. PEGDME is passed through a basic alumna column and diluted with diethyl ether solvent; the solution is stirred with molecular sieves for 24 h before removing solvent and drying under vacuum line at 50 °C for another 24 h. All other materials are purchased from Sigma-Aldrich and used directly.

Instrument. FTIR spectra are collected in a Mattson Galaxy 300 spectrometer. Thermogravimetric analyses (TGAs) are done under air using a PerkinElmer TGA 7. Transmission electron microscopy (TEM) on a JEOL-100CX instrument is used to characterize the morphology of the particles. Alternating current (AC) impedance spectroscopy conductivity data are collected from an HP 4192A LF impedance analyzer scanning from 5 Hz to 13 MHz with an applied voltage of 10 mV. The sample cell uses two steel disks as symmetrical electrodes separated by a Teflon collar, containing a sample of 0.61 cm in radii and 0.0175 cm in thickness. Samples are equilibrated at different temperatures for at least 10 min before measurement. Lithium quantitative analysis is done using Varian 710-ES inductively coupled plasma (ICP) optical emission spectrometer under argon atmosphere.

Synthesis. *Synthesis of Poly(sodium 4-styrenesulfonate)-Grafted Silica Nanoparticle (Si-PSSNa).* In a 50 mL Schlenk flask, 1.72 g of 4-styrenesulfonate (8.35 mmol), 56 mg of bipyridine (0.32 mmol), 6 mL of DI water, and 2 mL of methanol were mixed, being charged with a magnetic stir bar to stir to obtain a clear solution; a 0.124 g initiator-grafted silica nanoparticle was added; and the mixture was ultrasonicated for 15 min. After three cycles of freeze−pump−thaw, the Schlenk flask was filled with nitrogen and 17.2 mg of CuBr was added. After another cycle of freeze−pump−thaw, the reaction was done under room temperature for 12 h. The product is washed by DI water and *N,N,N′,N′*-ethylene diaminetetraacetic acid (disodium salt dehydrate, EDTA·2Na) saturated solution and then dried under vacuum at 90 °C overnight.

Lithiation of Poly(sodium 4-styrenesulfonate)-Grafted Silica Particle to Poly(lithium 4-styrenesulfonate)-Grafted Silica Particle (Si-PSSLi). In a 250 mL flask, 2.4 g of lithium chloride was dissolved in 100 mL of DI water. A 0.32 g amount of Si-PSSNa was added into the solution and ultrasonicated 15 min before reaction at room

DOI: 10.1021/acsami.5b05419
ACS Appl. Mater. Interfaces 2015, 7, 19335−19341

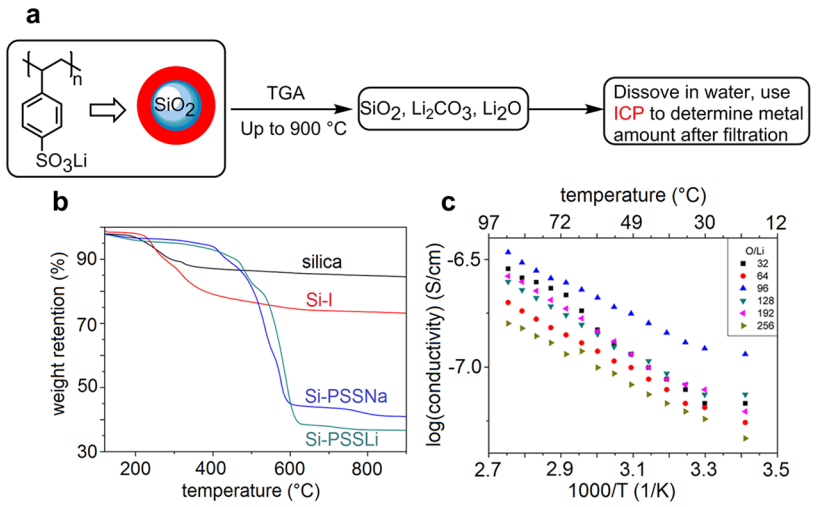

Figure 3. (a) Schematic description of the combined TGA and ICP technique to quantitatively characterize the lithium content in the polyelectrolyte-modified silica nanoparticles. (b) TGA of bare silica nanoparticles, Si-initiator, and Si-PSSLi. (c) Plots of conductivity as a function of inverse temperature for Si-PSSLi/PEGDME electrolytes at various O/Li ratios.

temperature for 48 h. Product was collected by centrifuge, washing by DI water, and drying under vacuum at 90 °C overnight.

Synthesis of Poly(sodium 4-styrenesulfonate) and Poly-PEGMA-Grafted Silica Nanoparticle (Si-PSSNa-PEGMA). in a 50 mL Schlenk flask, 1.72 g of 4-styrenesulfonate (6.26 mmol), 2.30 g of poly(ethylene glycol) ethyl ether methacrylate (2.09 mmol), 56 mg of bipyridine (0.32 mmol), 6 mL of DI water, and 2 mL of methanol were mixed, then being charged with a magnetic stir bar to stir to obtain a clear solution; a 0.124 g initiator-grafted silica nanoparticle was added; and the mixture was ultrasonicated for 15 min. After three cycles of freeze–pump–thaw, the Schlenk flask was filled with nitrogen and 17.2 mg of CuBr was added. After another cycle of freeze–pump–thaw, the reaction was done under room temperature for 12 h. Product was washed with DI water and *N,N,N′,N′*-ethylene diaminetetraacetic acid (disodium salt dehydrate, EDTA·2Na) saturated solution and then dried under vacuum at 90 °C overnight.

RESULTS AND DISCUSSION

Silica Nanoparticles Modified with Lithium 4-Styrenesulfonate (Si-PSSLi). The synthetic route to initiator-decorated nanoparticles (Si–I) is shown in Figure 2a. Synthesis of the attachable (11-(2-bromo-2-methyl)propionyloxy)-undecenyltrichlorosilane followed the procedure of Matyjaszewski et al.[29] The bromoisobutyryl structure is chemically bounded to the surface of silica particles, which is a very good initiating structure to trigger surface ATRP.[30−32]

Surface ATRP uses CuBr/bipyridine catalyst; poly(sodium 4-styrenesulfonate) brushes are grown from nanoparticles at room temperature. The poly(sodium 4-styrenesulfonate)-modified particles (Si-PSSNa) are converted to the corresponding Li^+ salt (Si-PSSLi) by reaction with lithium chloride solution (Figure 2a). The TEM image of Si-PSSLi (Figure 2b) shows that the particle diameter increases to 15–20 nm, compared to bare silica particles with 7–10 nm diameter. TEM characterization also shows that there is no significant aggregation of the particles.

Figure 2c shows FTIR spectra of the synthesized materials at different stages. The IR spectrum of bare silica particle shows a characteristic broad band centered at ∼790 cm^{-1} associated with Si–O and a strong and broad absorption band at 1150 cm^{-1}. In addition, there are C–H stretching bands at 2800–3000 cm^{-1} associated with cetyltrimethylammonium bromide (CTAB).[33,34] After anchoring the ATRP initiator (11-(2-bromo-2-methyl)propionyloxy)undecyltrichlorosilane to the nanoparticle surface, a new band appeared at 1730 cm^{-1} (C═O) as the initiator displaced the CTAB. The silica nanoparticles are received as well-dispersed in water solution; a surfactant such as CTAB is necessary to precipitate the silica particles, and thus a monolayer of CTAB might cover the particle surface, which is difficult to wash off. The IR spectrum of the poly(lithium 4-styrenesulfonate) brushes showed strong bands associated with the sulfonate group (S═O stretching, 1250, 1125 cm^{-1}) overtone/combination bands (1920 cm^{-1}) consistent with a 1,4-disubstituted aromatic ring and a significant increase in the C–H stretching bands (2800–3200 cm^{-1}). These data confirm successful growth of the polyelectrolyte from the surface.[35,36]

Figure 3b shows TGA curves for the synthesized composite material at different stages from 100 to 900 °C. Since the data are obtained in air, all organic components of the samples are oxidized to CO_2 and H_2O; the residual components are silica particles and other nonvolatile inorganic species. The bare silica particles have a weight loss of 15 wt % at 800 °C, which includes the loss of the CTAB surfactant residue, adsorbed water, and water formed by condensation of surface bound silanol groups. Assuming 10 nm diameter spherical SiO_2 particles (ρ = 2.6 g/cm^3) with a surface area of 300 m^2/g, a close packed monolayer of CTAB (cross-section of 0.8 nm^2), the expected mass loss due to CTAB is 16.5 wt %. A similar calculation for the initiator-modified particles predicts a weight loss of 15.1 wt %, assuming 0.6 nm^2/initiator chain,[17] although the actual weight loss for Si-initiator is higher at 27 wt %. After growing poly(sodium 4-styrenesulfonate) from the particles, the weight loss increases to 64 wt %. After lithium exchange, the weight loss increases to 72 wt %, consistent with the lower atomic weight of lithium.

Quantitative analysis of the TGA residue for lithium content provides an estimate of the number of anions bound to the nanoparticles (Figure 3a). Lithium in the TGA residue should be in the form of salts or metal oxides (Li_2O, Li_2O_2, and so on), which are water-soluble and can be analyzed by inductive coupled plasma (ICP) optical emission spectrometry. For the ICP analysis, the TGA residues are stirred in DI water for 12 h and filtered prior to the analysis. ICP analysis of the TGA

DOI: 10.1021/acsami.5b05419
ACS Appl. Mater. Interfaces 2015, 7, 19335−19341

residue from a 6.6 mg Si-PSSLi sample gives 0.16 mg of lithium, which corresponds to 2.4×10^{-2} g of Li/(g of sample). The data indicate that more than 95% of the Na ions are exchanged with Li ions; this enables formation of electrolytes with lithium content as high as 32/1 without an excessive amount of the inorganic particles in the Si-PSSLi/PEGDME composite. This lithium content is one to two orders higher than previous work with a monolayer of anions on the nanoparticles surface. By grafting polyanions on the nanoparticles, the samples contain high lithium content; we expect a good conductivity from this system. This combined TGA-ICP characterization method enables us to quantitatively characterize the lithium content of polyelectrolyte-grafted nanoparticles.

Homogeneous electrolytes with various O/Li ratios are prepared by dispersing polyelectrolyte-grafted silica nanoparticles in PEGDME. Figure 3c shows the Arrhenius plot of conductivities for the electrolytes at different O/Li ratios. With the initial addition of polyelectrolyte-modified silica nanoparticles into PEGDME, the conductivity is limited by the concentration of Li^+; thus the conductivity increases with the increase of Si-PSSLi. However, when the Si-PSSLi exceeded a particular amount, there were too many inorganic particles in the polymer matrix; not all the lithium sources can be fully used, and the composite also starts losing continuity. That causes the decrease of the conductivity. The conductivities extracted from the impedance spectroscopy data are roughly linear, consistent with thermal activated transport. The movement of ions is directly coupled to polymer chain mobility; this behavior is thermally activated and is often described by the Vogel–Tammann–Fulcher (VTF) equation[37−39]

$$\sigma = \sigma_0 \exp(-E_a(T - T_0))$$

where σ_0 is the pre-exponential factor related to the number of charge carriers, E_a is the apparent activation energy for ion transport, and T_0 is a parameter related to the chain mobility of the polymer. For polymers, low T_g should correlate to fast relaxation and high conductivity. Typically lithium transport is only limited to the amorphous regions. PEO, as the most widely used polymer electrolyte host, is featured for its high crystallization degree in solid state.[40] To avoid the influence of the PEO crystal and facilitate study of the polyelectrolyte-grafted silica nanoparticle/PEO system, we used PEO oligomer, which is in liquid state and does not have any crystallization region in the material.

Silica Nanoparticles Modified with Lithium 4-Styrenesulfonate and PEGMA (Si-PSSLi- PEGMA). Conductivities of the composite electrolyte based on Si-PSSLi at 60 °C are in the range of 10^{-7} S/cm; the highest value is 2.2×10^{-7} S/cm with O/Li of 96. The ionic conductivity of the composite electrolyte is much lower than expected. It is proposed that with a dense polyelectrolyte brush on the nanoparticles surface, most of the lithium ions are trapped in the inner part of the polyelectrolyte and do not contribute to the overall conductivity. Yameen et al. grew brushes from a mixture of oligo(ethylene glycol) and 2-sulfethyl methacrylate;[41] they obtained a 10^5 increase of the proton conductivity, which was ascribed to the hygroscopic oligo(ethylene glycol) chains. In a similar study, Schaefer et al. functionalized silica nanoparticle with PEG and sulfonate groups.[26] It is proposed that the tethered PEG functionalities could increase dissociation between lithium cation and sulfonate anion and improve solubility of the functionalized nanoparticles in tetraglyme solvent. In our study, diluting the sodium 4-styrenesulfonate phase with PEGMA facilitates lithium ion transport;[42] adding PEG chains to the particles could also improve the interface between the particles and the PEGDME host. To test these hypotheses and increase the conductivity, we co-polymerize PEGMA (M_n = 1100) with sodium 4-styrenesulfonate from the particle surface (Figure 4). The procedure for the surface-

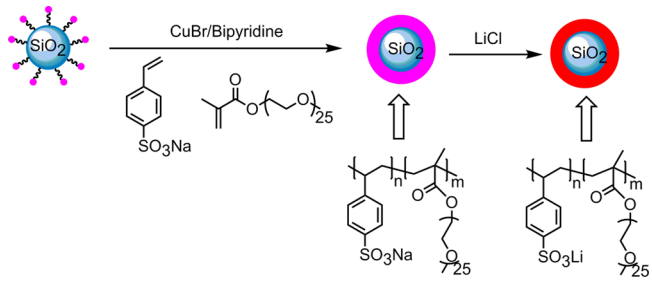

Figure 4. Co-polymerization of sodium 4-styrenesulfonate and PEGMA from silica nanoparticles (Si-PSSNa-PEGMA) and lithiation to Si-PSSLi-PEGMA.

initiated co-polymerization is similar to those used for the homopolymerization of sodium 4-styrenesulfonate. The molar ratio of sodium 4-styrenesulfonate to PEGMA monomers is 3/1, which corresponds to a polyelectrolyte with an O/Li ratio of 8/1. The ratio of the two monomers added to the particles can be calculated, since TGA provides the mass fraction of the organic phase on the particles, and ICP allows an estimate of the number of styrenesulfonate groups. The calculated value, 3.45/1, is close to the 3/1 feed ratio. Compared to styrene derivatives, methacrylate monomers have higher reactivity toward radical polymerization. However, the long PEG chain in PEGMA reduces the reactivity; thus we are able to obtain a co-polymer structure on the nanoparticle surface. Lithium exchange of Si-PSSNa-PEGMA was carried out using the same procedure as that for Si-PSSNa (Figure 4). The combined TGA-ICP analysis shows that lithiation efficiency is higher than 90% for different batches of materials. The Si-PSSLi-PEGMA sample used for making electrolytes has a lithium content of 1.6×10^{-2} g of Li/(g of sample).

The TEM shows particles with ∼15 nm diameter (Figure 5a). The IR spectrum of Si-PSSLi-PEGMA is shown in Figure 5b; signals corresponding to a PEG side structure are in the range of 1000−1200 cm^{-1}, which overlaps with PSSLi signals.[43] Figure 5c clearly shows that polyelectrolytes are grown from the nanoparticle surface, based on the considerable increase of weight loss. Since the PEGMA monomer used here has a molecular weight of ∼1100, after co-polymerization the composite nanoparticles have an increased organic component. TGA curves in Figure 5c show that Si-PSSNa-PEGMA has a weight loss of around 67% and Si-PSSLi-PEGMA has a weight loss of around 80%, compared to weigh loss of 64% for Si-PSSNa and 72% for Si-PSSLi. Figure 5d shows that the conductivities of the composite electrolytes based on Si-PSSLi-PEGMA increase with temperature. However, instead of a linear behavior for the Si-PSSLi sample shown in Figure 3c, the Si-PSSLi-PEGMA sample with PEO side chains incorporated shows a more curved behavior. A proposed explanation indicates that Si-PSSLi-PEGMA, on the other hand, may gradually release more Li^+ source in the internal polyelectrolyte shell with the increase of temperature; because the concentration of Li^+ changes during conductivity measurement, the

DOI: 10.1021/acsami.5b05419
ACS Appl. Mater. Interfaces 2015, 7, 19335−19341

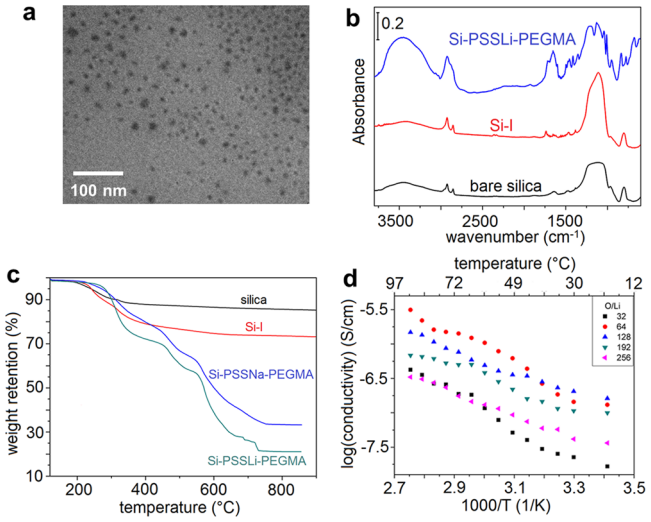

Figure 5. (a) TEM image of Si-PSSLi-PEGMA, (b) FTIR spectra, (c) TGA of bare silica nanoparticles, Si-initiator, and Si-PSSLi-PEGMA, and (d) plots of conductivity as a function of inverse temperature for Si-PSSLi-PEGMA/PEGDME electrolytes at various O/Li ratios.

VTF model is not applicable any more. Also, for Si-PSSLi-PEGMA, the highest conductivity at 60 °C is 1.3×10^{-6} S/cm at O/Li = 64; this value is almost an order higher than the composite electrolytes prepared from pure Si-PSSLi particles (2.2×10^{-7} S/cm). A proposed model in Figure 6 is used to explain the difference between Si-PSSLi and Si-PSSLi-PEGMA.

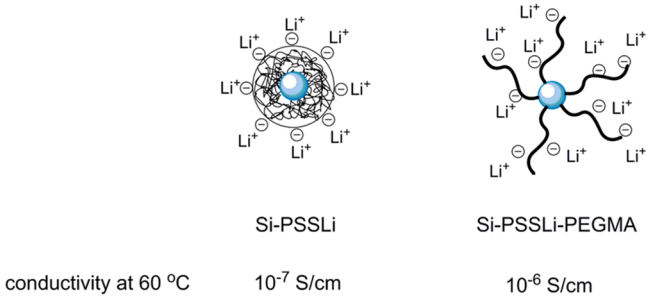

Figure 6. Proposed model for structural difference of Si-PSSLi and Si-PSSLi-PEGMA dispersed in PEGDME.

In the case of Si-PSSLi, polyelectrolyte itself does not have a good solubility in oligomer PEO, most of the polymer chains are collapsed on the nanoparticle surface; only the lithium cations in the outmost part could access the solvent and contribute to the conductivity, and that is why conductivity of Si-PSSLi is very low. PEGMA, on the other hand, has a long side chain with 25 repeating units of PEO; the bulky side groups are solvated by the solvent, which is oligomer PEO. The function of this structure is 2-fold: first, it helps to expand the dense polyelectrolyte brush on the nanoparticle surface (lithium ions inside the polyelectrolyte layer gain access to the oligomer PEO solvent and contribute to the conductivity); second, this long side chain on PEGMA also facilitates lithium ion mobility. We use AC impedance spectroscopy to measure the ionic conductivity of synthesized electrolyte materials; thus the reported conductivity data here are contributed to by all the ions in the electrolyte material.[44,45] Previous model studies indicate a polymer electrolyte with high lithium transference number holds great promise in preventing lithium dendrite formation.[46,47] The polyelectrolyte-grafted silica nanoparticles synthesized in this work represent a potential candidate that could enable the use of lithium metal in rechargeable batteries.

CONCLUSIONS

Nanocomposite lithium electrolytes are obtained by dispersing polyelectrolyte-grafted silica nanoparticles in oligomer PEO. A combined TGA-ICP characterization method enables us to quantitatively obtain the lithium content of polyelectrolyte-grafted nanoparticles; this lithium value is much higher compared to previous study with monolayer anion-grafted nanoparticles. Si-PSSLi gives moderate conductivity at 60 °C because of the poor solubility of polyanions in the solvent. Si-PSSLi-PEGMA has PEGMA, with a long PEO side chain in the polymer backbone; there is an order increase of the conductivity to $\sim 10^{-6}$ S/cm. Other polyelectrolyte and anion structures that give better dissociation of ions could potentially improve the conductivity. Also, the use of other solvents with high dielectric constants, such as ethylene carbonate ($\varepsilon \approx 90$), propylene carbonates ($\varepsilon \approx 65$), and ionic liquids, should further improve the conductivity.

ASSOCIATED CONTENT

Supporting Information

The Supporting Information is available free of charge on the ACS Publications website at DOI: 10.1021/acsami.5b05419.

Detail about electrochemical data of PEGDME/LiTFSI (PDF)

AUTHOR INFORMATION

Corresponding Author

*Tel.: +1 510 486 7207. Fax: +1 510 486 7303. E-mail: gliu@lbl.gov.

Author Contributions

§H.Z. and Z.J. contributed equally to this work

Notes

The authors declare no competing financial interest.

ACKNOWLEDGMENTS

This work was funded by the Assistant Secretary for Energy Efficiency, Vehicle Technologies Office of the U.S. Department of Energy (U.S. DOE) under the Advanced Battery Materials Research (BMR) and Applied Battery Research (ABR) Programs, supported by the U.S. Department of Energy under Contract No. DE-AC02-05 CH11231. We thank the Michigan State University (MSU) Center for Alternative Energy Storage Research and Technology (CAESRT) and the U.S. Army Research Office. Professor Baker passed away in October 2012; this work is dedicated to him.

ABBREVIATIONS

PEGDME, polyethylene glycol dimethyl ether with M_w = 500 g/mol

PEGMA, poly(ethylene oxide) methacrylate

Si-PSSLi, silica nanoparticles grafted with poly(lithium 4-styrenesulfonate)

Si-PSSLi-PEGMA, silica nanoparticles grafted with copoly-(lithium 4-styrenesulfonate)-PEGMA

DOI: 10.1021/acsami.5b05419
ACS Appl. Mater. Interfaces 2015, 7, 19335−19341

REFERENCES

(1) Goodenough, J. B.; Kim, Y. Challenges for Rechargeable Li Batteries. *Chem. Mater.* **2010**, *22*, 587−603.

(2) Zhao, H.; Zhou, X.; Park, S.-J.; Shi, F.; Fu, Y.; Ling, M.; Yuca, N.; Battaglia, V.; Liu, G. A Polymerized Vinylene Carbonate Anode Binder Enhances Performance of Lithium-ion Batteries. *J. Power Sources* **2014**, *263*, 288−295.

(3) Zhao, H.; Yuan, W.; Liu, G. Hierarchical Electrode Design of High-Capacity Alloy Nanomaterials for Lithium-Ion Batteries. *Nano Today* **2015**, *10*, 193−212.

(4) Zhao, H.; Wang, Z.; Lu, P.; Jiang, M.; Shi, F.; Song, X.; Zheng, Z.; Zhou, X.; Fu, Y.; Abdelbast, G.; Xiao, X.; Liu, Z.; Battaglia, V. S.; Zaghib, K.; Liu, G. Toward Practical Application of Functional Conductive Polymer Binder for a High-Energy Lithium-Ion Battery Design. *Nano Lett.* **2014**, *14*, 6704−6710.

(5) Park, S.-J.; Zhao, H.; Ai, G.; Wang, C.; Song, X.; Yuca, N.; Battaglia, V. S.; Yang, W.; Liu, G. Side-Chain Conducting and Phase-Separated Polymeric Binders for High-Performance Silicon Anodes in Lithium-Ion Batteries. *J. Am. Chem. Soc.* **2015**, *137*, 2565−2571.

(6) Feng, C.; Zhang, L.; Yang, M.; Song, X.; Zhao, H.; Jia, Z.; Sun, K.; Liu, G. One-Pot Synthesis of Copper Sulfide Nanowires/Reduced Graphene Oxide Nanocomposites with Excellent Lithium-Storage Properties as Anode Materials for Lithium-Ion Batteries. *ACS Appl. Mater. Interfaces* **2015**, *7*, 15726−15734.

(7) Bruce, P. G.; Freunberger, S. A.; Hardwick, L. J.; Tarascon, J.-M. Li−O2 and Li−S Batteries with High Energy Storage. *Nat. Mater.* **2012**, *11*, 19−29.

(8) Vaughey, J. T.; Liu, G.; Zhang, J.-G. Stabilizing the Surface of Lithium Metal. *MRS Bull.* **2014**, *39*, 429−435.

(9) Shi, F.; Zhao, H.; Liu, G.; Ross, P. N.; Somorjai, G. A.; Komvopoulos, K. Identification of Diethyl 2,5-Dioxahexane Dicarboxylate and Polyethylene Carbonate as Decomposition Products of Ethylene Carbonate Based Electrolytes by Fourier Transform Infrared Spectroscopy. *J. Phys. Chem. C* **2014**, *118*, 14732−14738.

(10) Shi, F.; Ross, P. N.; Zhao, H.; Liu, G.; Somorjai, G. A.; Komvopoulos, K. A Catalytic Path for Electrolyte Reduction in Lithium-Ion Cells Revealed by in Situ Attenuated Total Reflection-Fourier Transform Infrared Spectroscopy. *J. Am. Chem. Soc.* **2015**, *137*, 3181−3184.

(11) Harry, K. J.; Hallinan, D. T.; Parkinson, D. Y.; MacDowell, A. A.; Balsara, N. P. Detection of Subsurface Structures Underneath Dendrites Formed on Cycled Lithium Metal Electrodes. *Nat. Mater.* **2014**, *13*, 69−73.

(12) Ding, F.; Xu, W.; Graff, G. L.; Zhang, J.; Sushko, M. L.; Chen, X.; Shao, Y.; Engelhard, M. H.; Nie, Z.; Xiao, J.; Liu, X.; Sushko, P. V.; Liu, J.; Zhang, J.-G. Dendrite-Free Lithium Deposition via Self-Healing Electrostatic Shield Mechanism. *J. Am. Chem. Soc.* **2013**, *135*, 4450−4456.

(13) Ding, F.; Xu, W.; Chen, X.; Zhang, J.; Shao, Y.; Engelhard, M. H.; Zhang, Y.; Blake, T. A.; Graff, G. L.; Liu, X.; Zhang, J.-G. Effects of Cesium Cations in Lithium Deposition via Self-Healing Electrostatic Shield Mechanism. *J. Phys. Chem. C* **2014**, *118*, 4043−4049.

(14) Zheng, G.; Lee, S. W.; Liang, Z.; Lee, H.-W.; Yan, K.; Yao, H.; Wang, H.; Li, W.; Chu, S.; Cui, Y. Interconnected Hollow Carbon Nanospheres for Stable Lithium Metal Anodes. *Nat. Nanotechnol.* **2014**, *9*, 618−623.

(15) Armand, M. B.; Chabagno, J. M.; Duclot, M. *Second International Meeting on Solid Electrolytes*, University of St Andrews, Scotland; University of St Andrews, Fife, Scotland, 1978.

(16) Chazalviel, J. N. Electrochemical Aspects of the Generation of Ramified Metallic Electrodeposits. *Phys. Rev. A: At., Mol., Opt. Phys.* **1990**, *42*, 7355−7367.

(17) Zhao, H.; Park, S.-J.; Shi, F.; Fu, Y.; Battaglia, V.; Ross, P. N.; Liu, G. Propylene Carbonate (PC)-Based Electrolytes with High Coulombic Efficiency for Lithium-Ion Batteries. *J. Electrochem. Soc.* **2014**, *161*, A194−A200.

(18) Alloin, F.; Sanchez, J. Y.; Armand, M. B. Conductivity Measurements of LiTFSI Triblock Copolymers with a Central POE Sequence. *Electrochim. Acta* **1992**, *37*, 1729−1731.

(19) Quartarone, E.; Mustarelli, P. Electrolytes for Solid-State Lithium Rechargeable Batteries: Recent Advances and Perspectives. *Chem. Soc. Rev.* **2011**, *40*, 2525−2540.

(20) Fujinami, T.; Tokimune, A.; Mehta, M. A.; Shriver, D. F.; Rawsky, G. C. Siloxyaluminate Polymers with High Li+ Ion Conductivity. *Chem. Mater.* **1997**, *9*, 2236−2239.

(21) Snyder, J. F.; Hutchison, J. C.; Ratner, M. A.; Shriver, D. F. Synthesis of Comb Polysiloxane Polyelectrolytes Containing Oligoether and Perfluoroether Side Chains. *Chem. Mater.* **2003**, *15*, 4223−4230.

(22) Sun, X.-G.; Reeder, C. L.; Kerr, J. B. Synthesis and Characterization of Network Type Single Ion Conductors. *Macromolecules* **2004**, *37*, 2219−2227.

(23) Sun, X.-G.; Kerr, J. B. Synthesis and Characterization of Network Single Ion Conductors Based on Comb-Branched Polyepoxide Ethers and Lithium Bis(allylmalonato)borate. *Macromolecules* **2006**, *39*, 362−372.

(24) Matsumoto, K.; Endo, T. Synthesis of Ion Conductive Networked Polymers Based on an Ionic Liquid Epoxide Having a Quaternary Ammonium Salt Structure. *Macromolecules* **2009**, *42*, 4580−4584.

(25) Zhang, X.-W.; Fedkiw, P. S. Ionic Transport and Interfacial Stability of Sulfonate-Modified Fumed Silicas as Nanocomposite Electrolytes. *J. Electrochem. Soc.* **2005**, *152*, A2413−A2420.

(26) Schaefer, J. L.; Yanga, D. A.; Archer, L. A. High Lithium Transference Number Electrolytes via Creation of 3-Dimensional, Charged, Nanoporous Networks from Dense Functionalized Nanoparticle Composites. *Chem. Mater.* **2013**, *25*, 834−839.

(27) Qin, J.; Zhao, H.; Liu, X.; Zhang, X.; Gu, Y. Double Phase Separation in Preparing Polyimide/Silica Hybrid Films by Sol−Gel Method. *Polymer* **2007**, *48*, 3379−3383.

(28) Qin, J.; Zhao, H.; Zhu, R.; Zhang, X.; Gu, Y. Effect of Chemical Interaction on Morphology and Mechanical Properties of CPI-OH/SiO2 Hybrid Films with Coupling Agent. *J. Appl. Polym. Sci.* **2007**, *104*, 3530−3538.

(29) Matyjaszewski, K.; Miller, P. J.; Shukla, N.; Immaraporn, B.; Gelman, A.; Luokala, B. B.; Siclovan, T. M.; Kickelbick, G.; Vallant, T.; Hoffmann, H.; Pakula, T. Polymers at Interfaces: Using Atom Transfer Radical Polymerization in the Controlled Growth of Homopolymers and Block Copolymers from Silicon Surfaces in the Absence of Untethered Sacrificial Initiator. *Macromolecules* **1999**, *32*, 8716−8724.

(30) Yuan, W.; Zhao, H.; Hu, H.; Wang, S.; Baker, G. L. Synthesis and Characterization of the Hole-Conducting Silica/Polymer Nanocomposites and Application in Solid-State Dye-Sensitized Solar Cell. *ACS Appl. Mater. Interfaces* **2013**, *5*, 4155−4161.

(31) Hu, H.; Yuan, W.; Zhao, H.; Baker, G. L. A Novel Polymer Gel Electrolyte: Direct Polymerization of Ionic Liquid from Surface of Silica Nanoparticles. *J. Polym. Sci., Part A: Polym. Chem.* **2014**, *52*, 121−127.

(32) Jia, Z.; Yuan, W.; Sheng, C.; Zhao, H.; Hu, H.; Baker, G. L. Optimizing the Electrochemical Performance of Imidazolium-Based Polymeric Ionic Liquids by Varying Tethering Groups. *J. Polym. Sci., Part A: Polym. Chem.* **2015**, *53*, 1339−1350.

(33) Jia, Z.; Yuan, W.; Zhao, H.; Hu, H.; Baker, G. L. Composite Electrolytes Comprised of Poly(ethylene oxide) and Silica Nanoparticles with Grafted Poly(ethylene oxide)-Containing Polymers. *RSC Adv.* **2014**, *4*, 41087−41098.

(34) Hu, H.; Yuan, W.; Lu, L.; Zhao, H.; Jia, Z.; Baker, G. L. Low Glass Transition Temperature Polymer Electrolyte Prepared from Ionic Liquid Grafted Polyethylene Oxide. *J. Polym. Sci., Part A: Polym. Chem.* **2014**, *52*, 2104−2110.

(35) Ling, M.; Qiu, J.; Li, S.; Zhao, H.; Liu, G.; Zhang, S. An Environmentally Benign LIB Fabrication Process Using a Low Cost, Water Soluble and Efficient Binder. *J. Mater. Chem. A* **2013**, *1*, 11543−11547.

(36) Ling, M.; Xu, Y.; Zhao, H.; Gu, X.; Qiu, J.; Li, S.; Wu, M.; Song, X.; Yan, C.; Liu, G.; Zhang, S. Dual-Functional Gum Arabic Binder for Silicon Anodes in Lithium Ion Batteries. *Nano Energy* **2015**, *12*, 178−185.

DOI: 10.1021/acsami.5b05419
ACS Appl. Mater. Interfaces 2015, 7, 19335−19341

(37) Vogel, H. The Temperature Dependence of the Viscosity of Liquids. *Phys. Z.* **1921**, *22*, 645−646.
(38) Tammann, G.; Hesse, W. Z. The Dependence of Viscosity on Temperature of Supercooled Liquids. *Z. Anorg. Allg. Chem.* **1926**, *156*, 245−257.
(39) Fulcher, G. S. Analysis of Recent Measurement of the Viscosity of Glasses. *J. Am. Ceram. Soc.* **1925**, *8*, 339−355.
(40) Khurana, R.; Schaefer, J. L.; Archer, L. A.; Coates, G. W. Suppression of Lithium Dendrite Growth Using Cross-Linked Polyethylene/Poly(ethylene oxide) Electrolytes: A New Approach for Practical Lithium-Metal Polymer Batteries. *J. Am. Chem. Soc.* **2014**, *136*, 7395−7402.
(41) Yameen, B.; Kaltbeitzel, A.; Langer, A.; Muller, F.; Gosele, U.; Knoll, W.; Azzaroni, O. Highly Proton-Conducting Self-Humidifying Microchannels Generated by Copolymer Brushes on a Scaffold. *Angew. Chem. Int. Ed.* **2009**, *48*, 3124−3128.
(42) Yuca, N.; Zhao, H.; Song, X.; Dogdu, M. F.; Yuan, W.; Fu, Y.; Battaglia, V. S.; Xiao, X.; Liu, G. A Systematic Investigation of Polymer Binder Flexibility on the Electrode Performance of Lithium-Ion Batteries. *ACS Appl. Mater. Interfaces* **2014**, *6*, 17111−17118.
(43) Ling, M.; Zhao, H.; Xiaoc, X.; Shi, F.; Wu, M.; Qiu, J.; Li, S.; Song, X.; Liu, G.; Zhang, S. Low Cost and Environmentally Benign Crack-Blocking Structures for Long Life and High Power Si Electrodes in Lithium Ion Batteries. *J. Mater. Chem. A* **2015**, *3*, 2036−2042.
(44) Yuan, W.; Wu, M.; Zhao, H.; Song, X.; Liu, G. Baseline Si Electrode Fabrication and Performance for the Battery for Advanced Transportation Technologies Program. *J. Power Sources* **2015**, *282*, 223−227.
(45) Dai, K.; Zhao, H.; Wang, Z.; Song, X.; Battaglia, V.; Liu, G. Toward High Specific Capacity and High Cycling Stability of Pure Tin Nanoparticles with Conductive Polymer Binder for Sodium Ion Batteries. *J. Power Sources* **2014**, *263*, 276−279.
(46) Doyle, M.; Fuller, T. F.; Newman, J. The Importance of the Lithium Ion Transference Number in Lithium/Polymer Cells. *Electrochim. Acta* **1994**, *39*, 2073−2081.
(47) Monroe, C.; Newman, J. Dendrite Growth in Lithium/Polymer Systems: A Propagation Model for Liquid Electrolytes under Galvanostatic Conditions. *J. Electrochem. Soc.* **2003**, *150*, A1377−A1384.

DOI: 10.1021/acsami.5b05419
ACS Appl. Mater. Interfaces 2015, 7, 19335−19341